Supplementary Material (ESI) for *PCCP*

Adsorption-Desorption and Photocatalytic Properties of Inorganic Organic Hybrid Cadmium Thiosulfate Compounds

Avijit Kumar Paul[a], Giridhar Madras[b*] and Srinivasan Natarajan[a*]

[a] Framework Solids Laboratory, Solid State and Structural Chemistry Unit, Indian Institute of Science, Bangalore-560012, India. E-mail: snatarajan@sscu.iisc.ernet.in

[b] Department of Chemical Engineering, Indian Institute of Science, Bangalore-560012, India.

E-mail: giridhar@chemeng.iisc.ernet.in

ELECTRONIC SUPPORTING INFORMATION

Figure S1: Structure of all the investigated dyes.

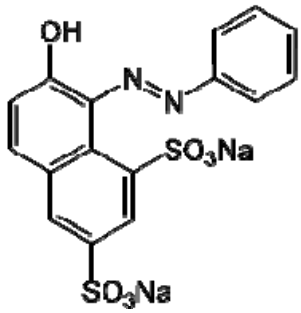

Orange G (OG)

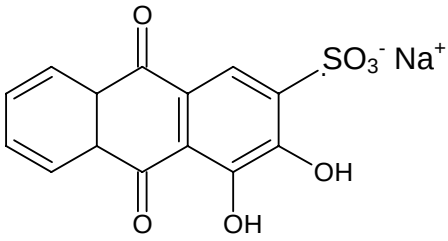

Alizarin Red S (AZS)

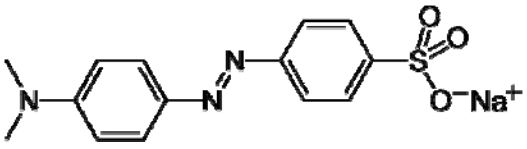

Methyl Orange (MO)

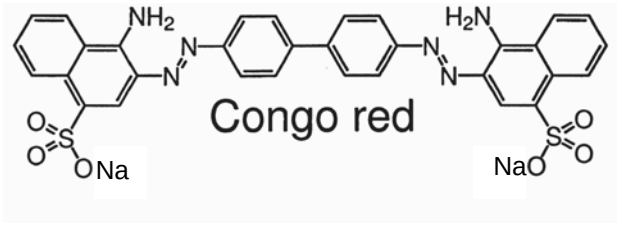

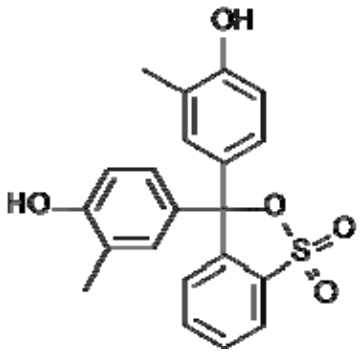

Cresol Red (CRR)

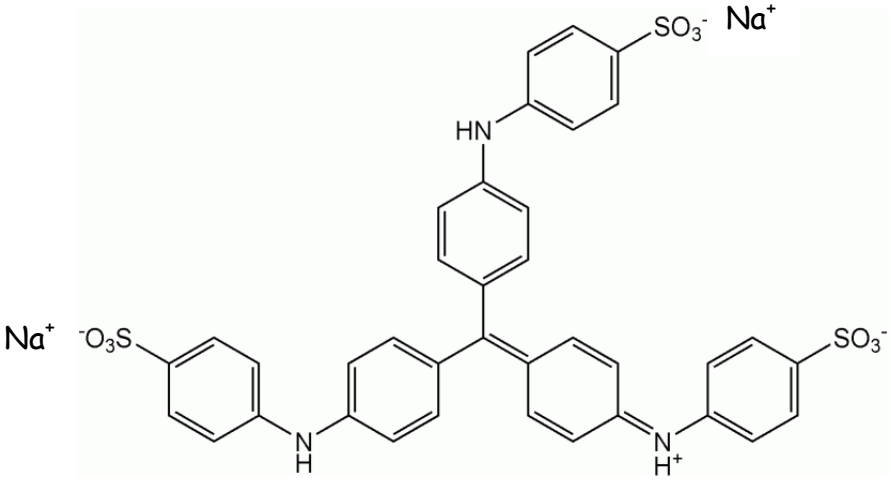

Cotton Blue (CB)

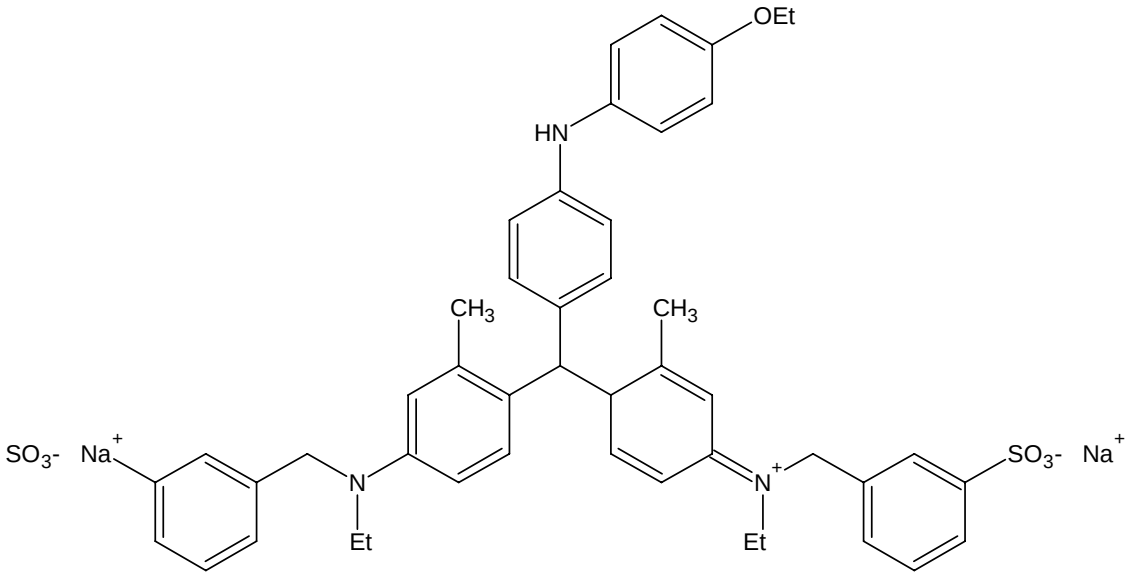

Comassie Blue (CBB)

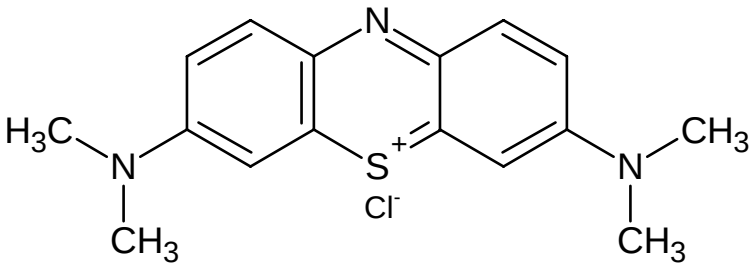

Methylene Blue (MB)

Supplementary Material (ESI) for *PCCP*

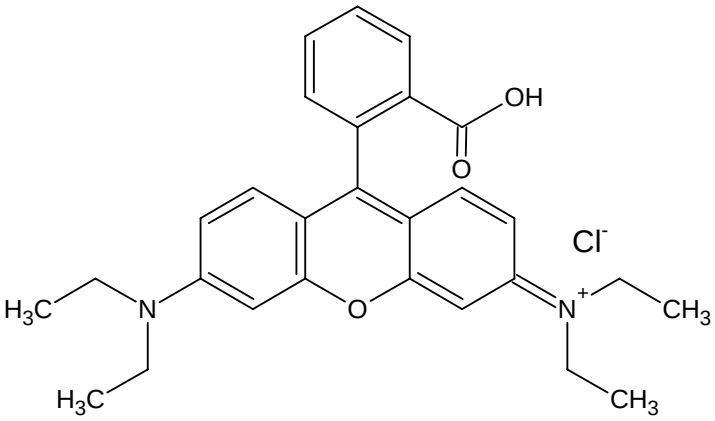

Rhodamine Blue (RBL)

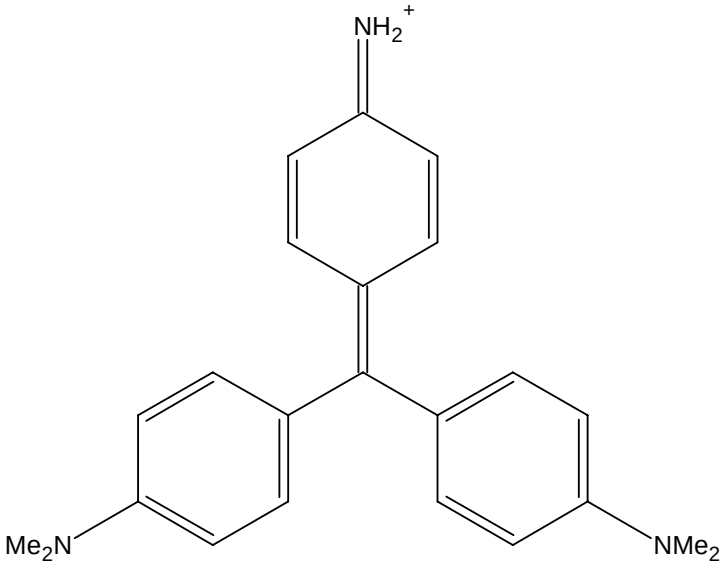

Methyl Violet (MV)

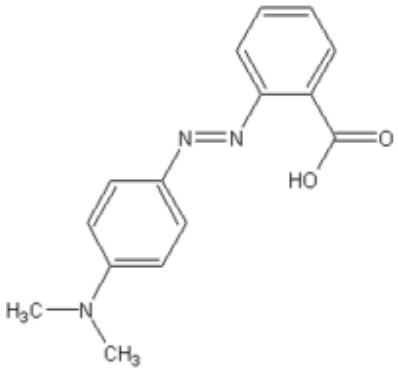

Methyl Red (MR)

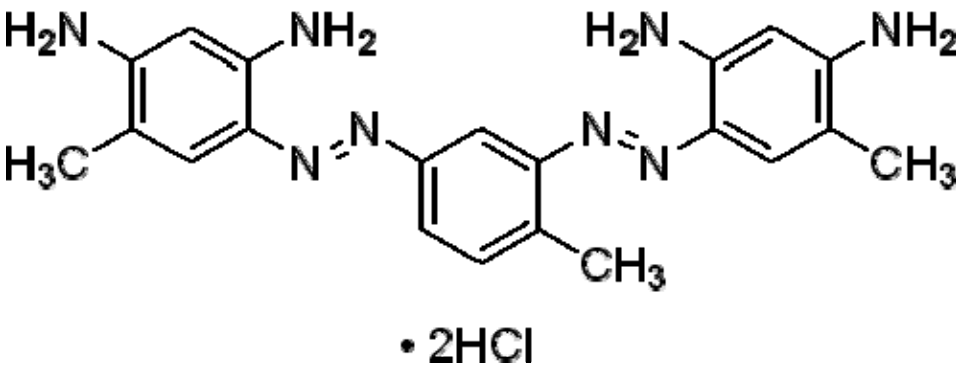

Bismarck Brown R (BBR)

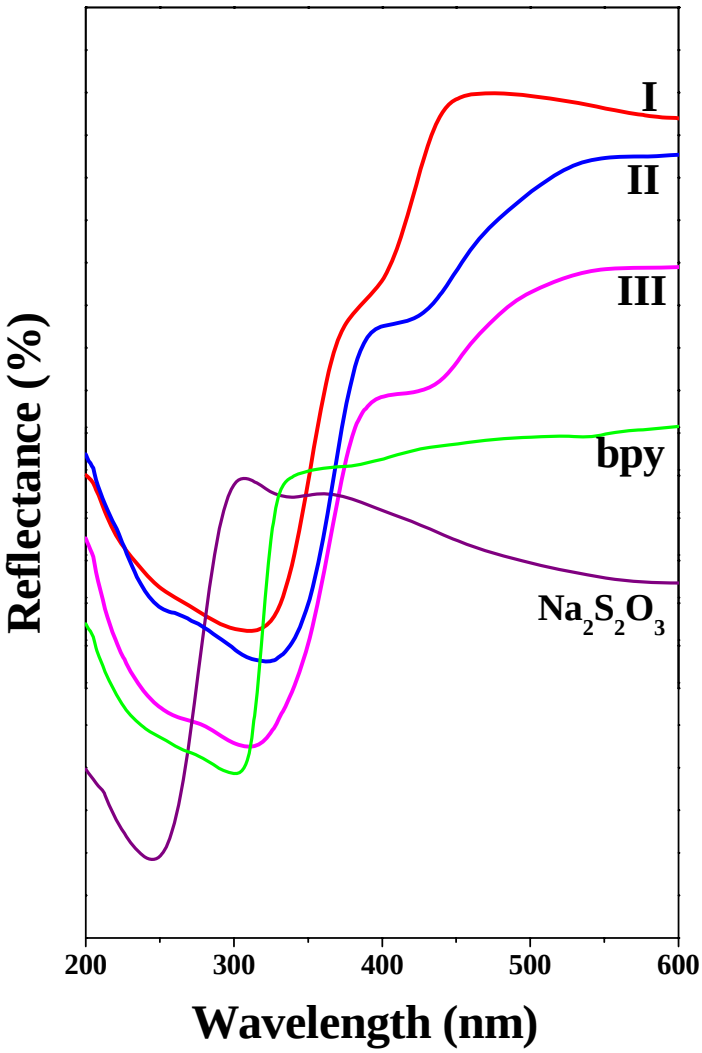

Fig. S2: Solid state UV-visible reflectance spectra of $Na_2S_2O_3$, 4,4'-bipyridine and compounds **I-III.**

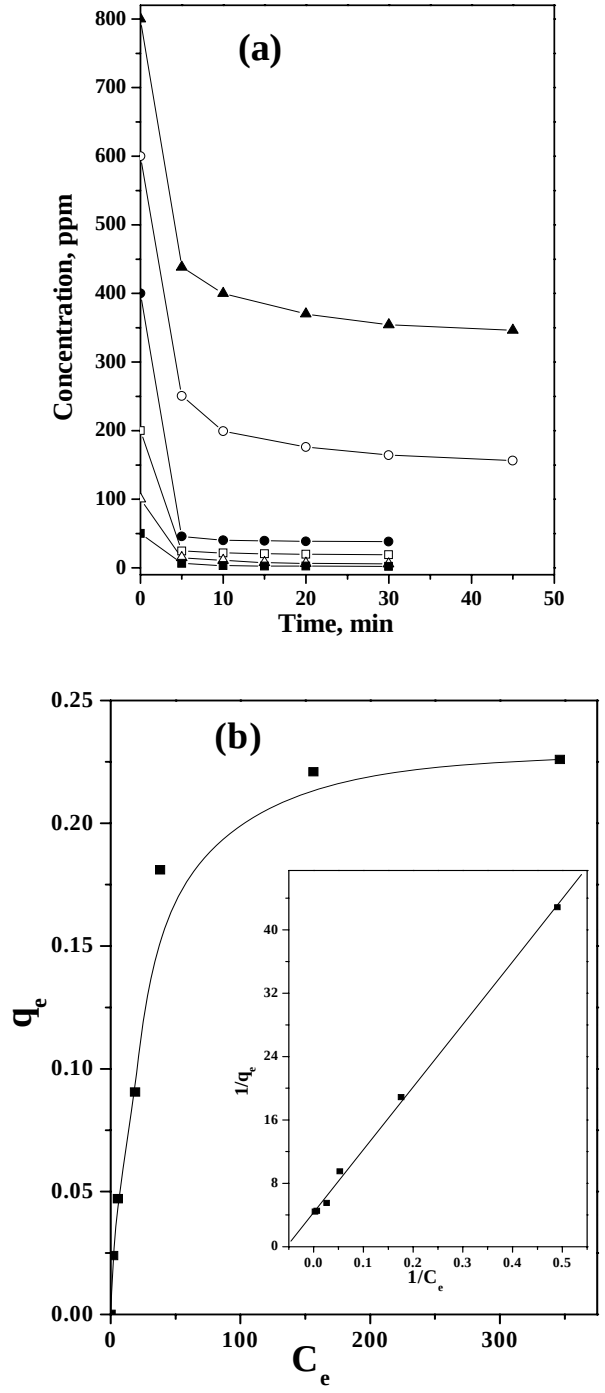

Fig. S3: (a) Adsorption profiles of OG with the different initial concentrations in the presence of 2 g/l of **I.** (▼ = 800 ppm, o = 600 ppm, ● = 400 ppm, □ = 200 ppm, Δ = 100 ppm, ■ = 50 ppm).

(b) The profile of the variation of the equilibrium adsorption (q_e) with equilibrium concentration (C_e) of OG. Inset shows $1/q_e$ vs $1/C_e$ plot.

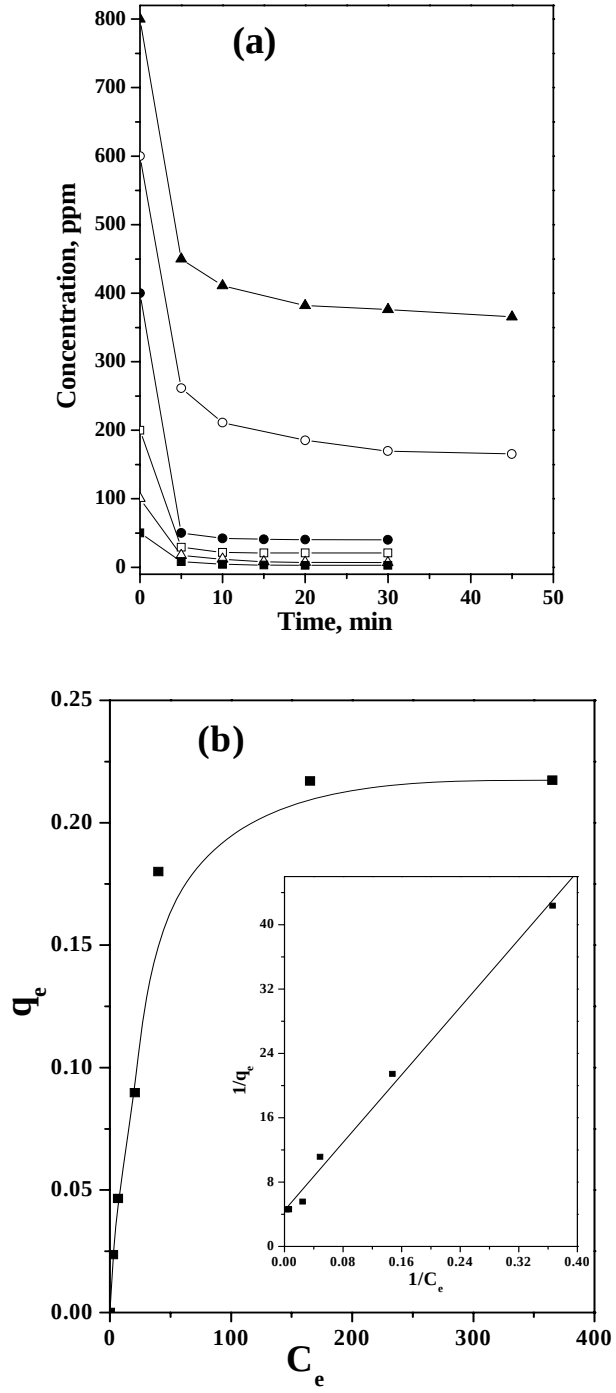

Fig. S4: (a) Adsorption profiles of OG with the different initial concentrations in the presence of **III.** (▼ = 800 ppm, o = 600 ppm, ● = 400 ppm, □ = 200 ppm, Δ = 100 ppm, ■ = 50 ppm).

(b) The profile of the variation of the equilibrium adsorption (q_e) with equilibrium concentration (C_e) of OG. Inset shows $1/q_e$ vs $1/C_e$ plot.

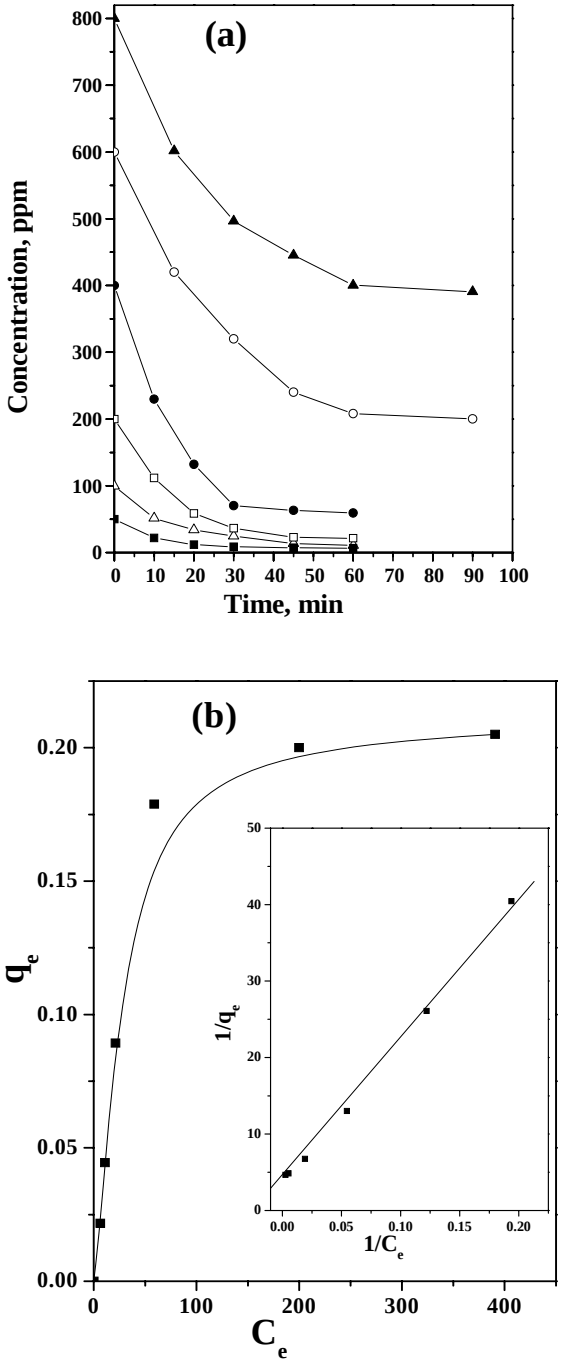

Fig. S5: (a) Adsorption profiles of ARS with the different initial concentrations in presence of 2 g/l of **I .**

(▼ = 800 ppm, o = 600 ppm, ● = 400 ppm, □ = 200 ppm, Δ = 100 ppm, ■ = 50 ppm).

(b) The profile of the variation of the equilibrium adsorption (q_e) with equilibrium concentration (C_e) of ARS. Inset shows $1/q_e$ vs $1/C_e$ plot.

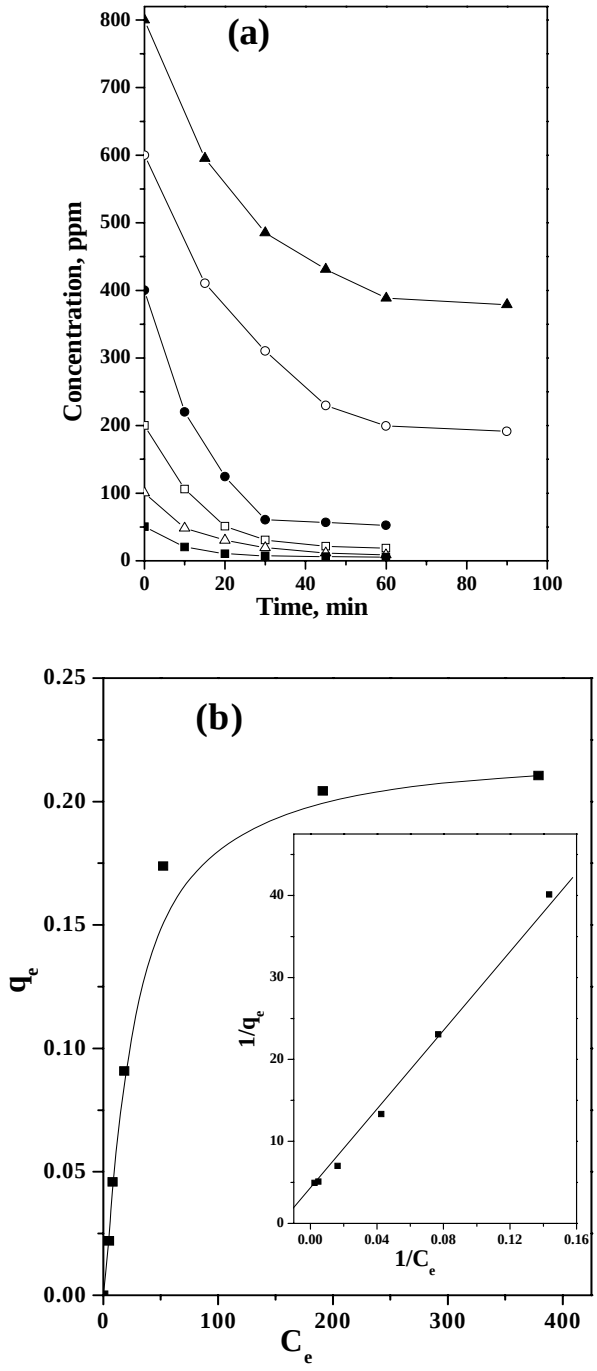

Fig. S6: (a) Adsorption profiles of ARS with the different initial concentrations in the presence of **III.**

(▼ = 800 ppm, o = 600 ppm, ● = 400 ppm, □ = 200 ppm, Δ = 100 ppm, ■ = 50 ppm).

(b) The profile of the variation of the equilibrium adsorption (q_e) with equilibrium concentration (C_e) of ARS. Inset shows $1/q_e$ vs $1/C_e$ plot.

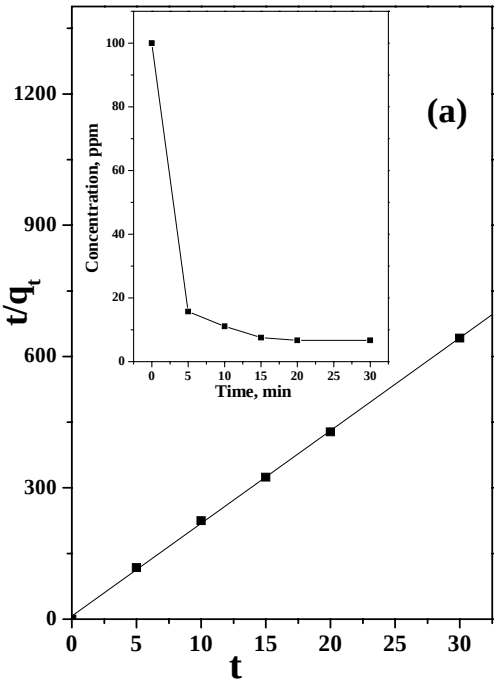

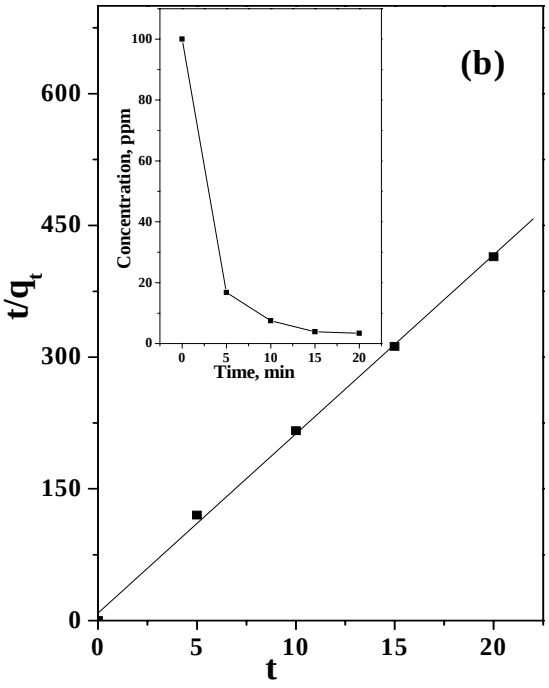

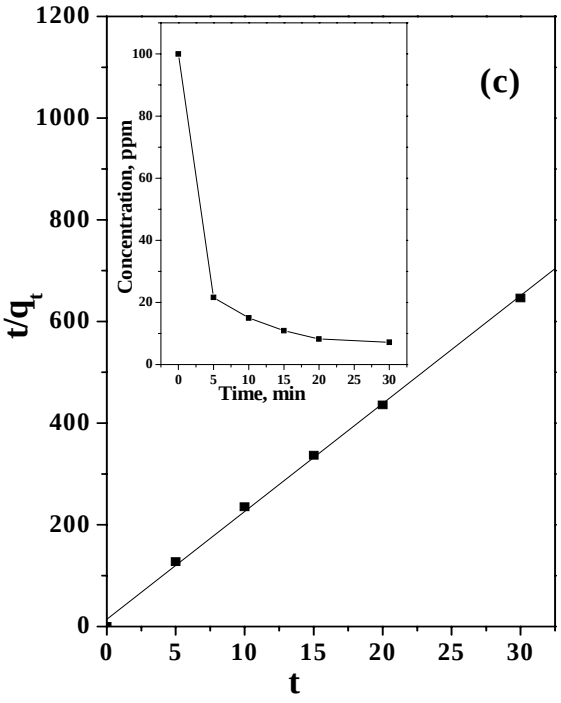

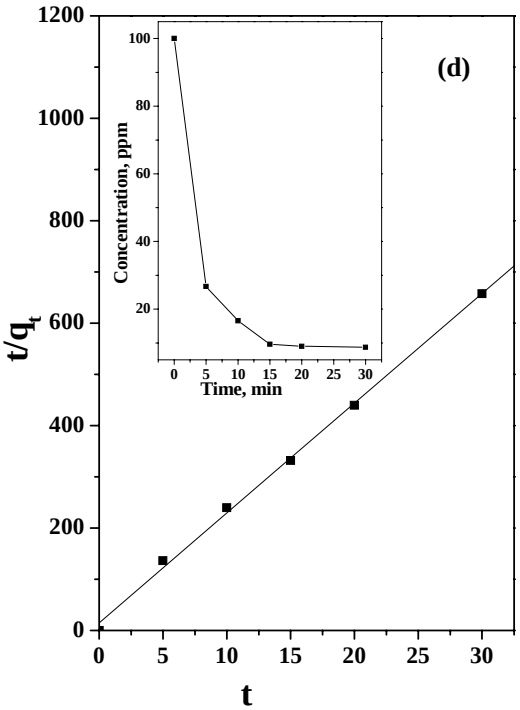

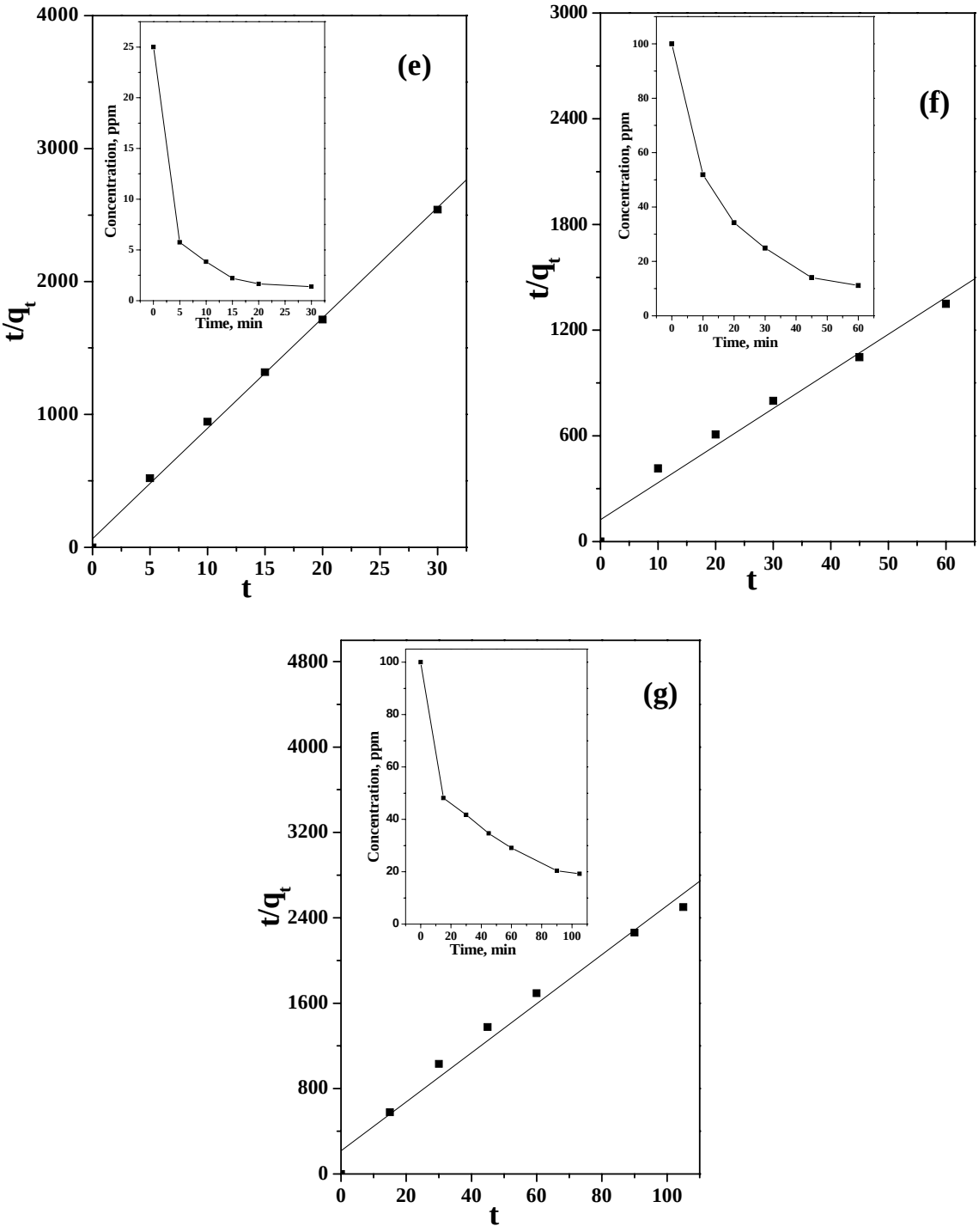

Fig. S7. The linear plot of adsorbed dye concentration with the function of time for different sulfonated dyes (a) OG, (b) CR, (c) CB, (d) MO, (e) CRR, (f) ARS and (g) CBB for 2 g/l of **II**. Inset shows the change of concentration of the respective dyes with variation of time.

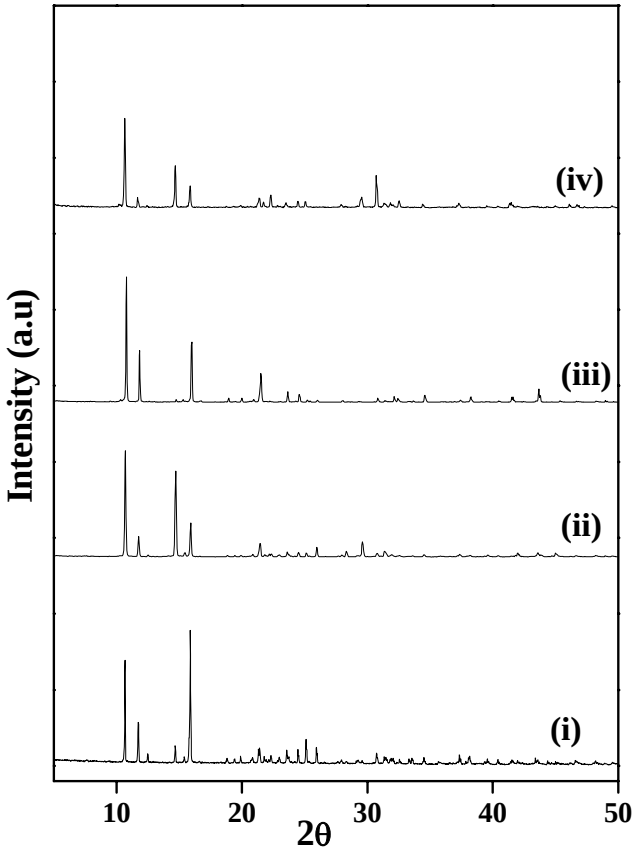

Fig. S8. PXRD pattern of (i) **II** and compound **II** after the adsorption of dyes (ii) OG (iii) ARS and (iv) CBB.

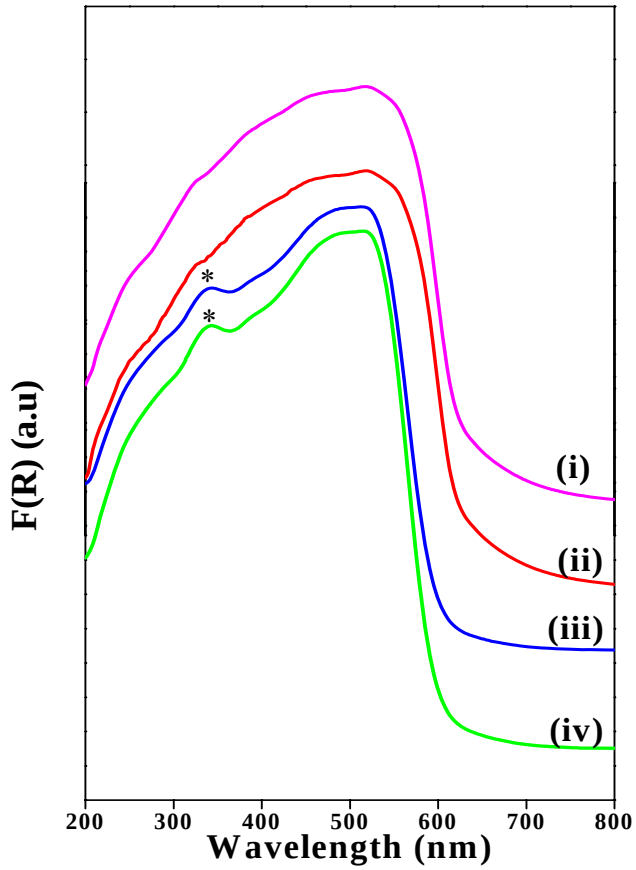

Fig. S9. Solid state UV-vis absorbance like spectra for (i) OG (ii) OG after exposing in UV light for 1 hour (iii) compound **II** after adsorption of OG (iv) compound **II** after adsorption of OG and exposed to UV light for 1 hour. (* represents the absorbance peak of **II** due to the intra-ligand electron transfer)

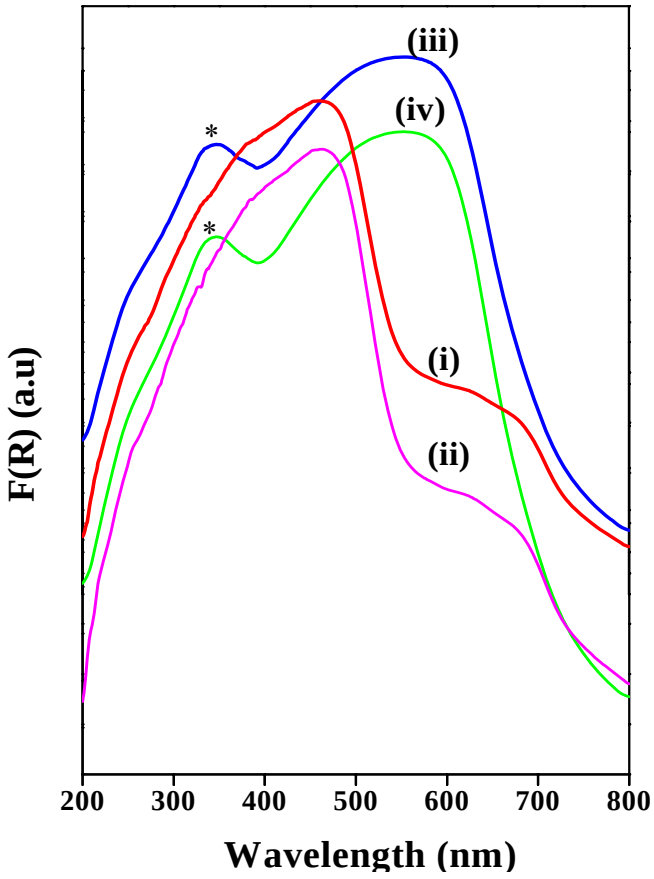

Fig. S10. Solid state UV-vis absorbance like spectra for (i) ARS (ii) ARS after exposing in UV light for 1 hour (iii) compound **II** after adsorption of ARS (iv) compound **II** after adsorption of ARS and exposed to UV light for 1 hour. (∗ represents the absorbance peak of **II** due to the intra-ligand electron transfer).

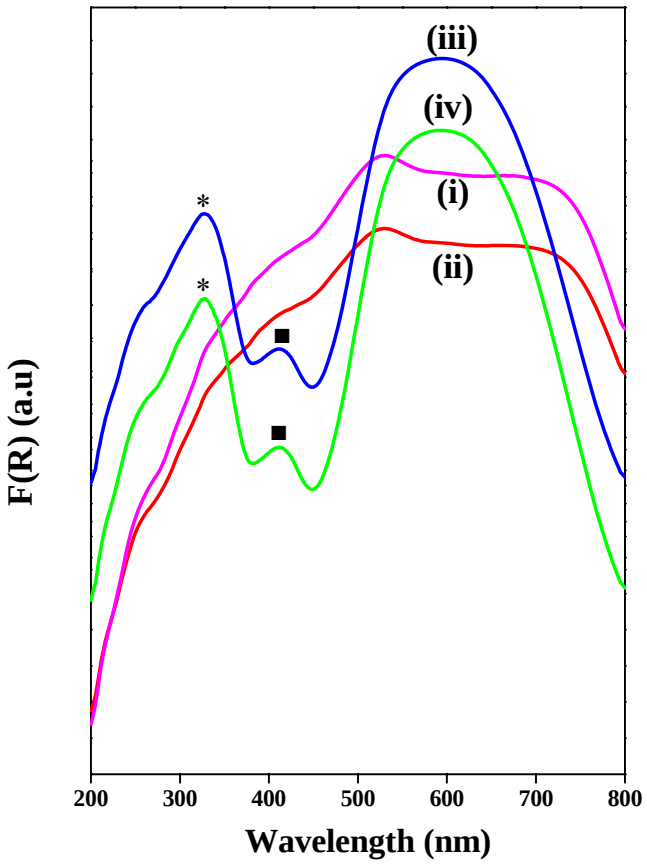

Fig. S11. Solid state UV-vis absorbance like spectra for (i) CBB (ii) CBB after exposing in UV light for 1 hour (iii) compound **II** after adsorption of CBB (iv) compound **II** after adsorption of CBB and exposed to UV light for 1 hour. (∗ represents the absorbance peak due to the intra-ligand electron transfer and ■ represents the absorbance peak due to ligand-metal charge transfer of **II**).

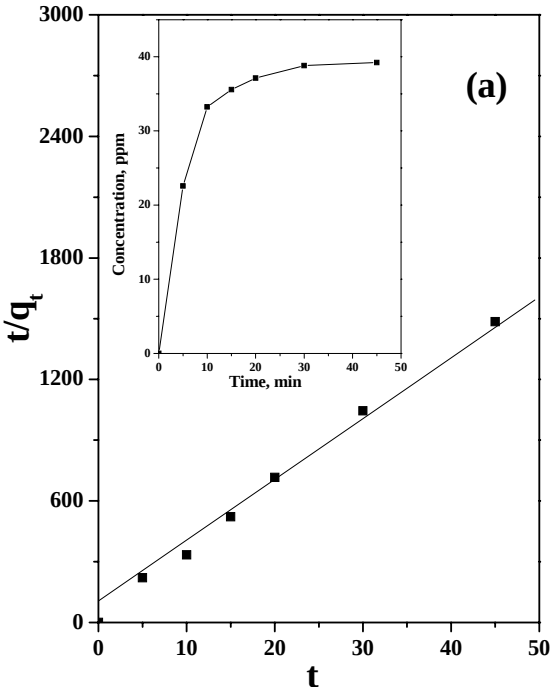

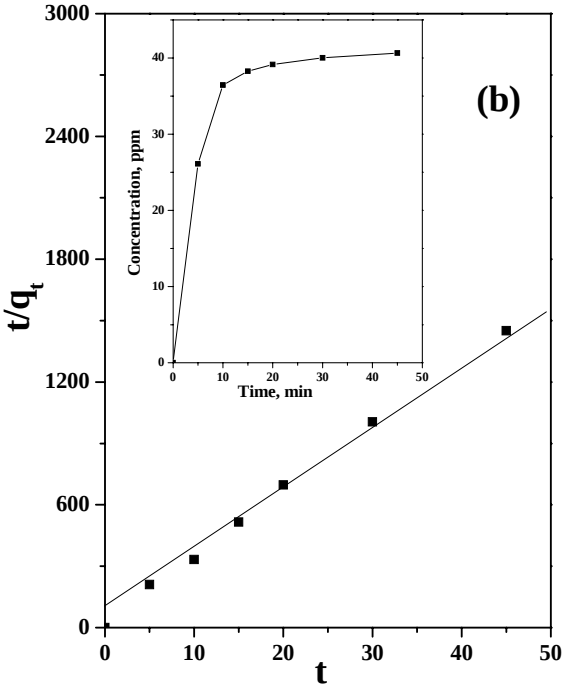

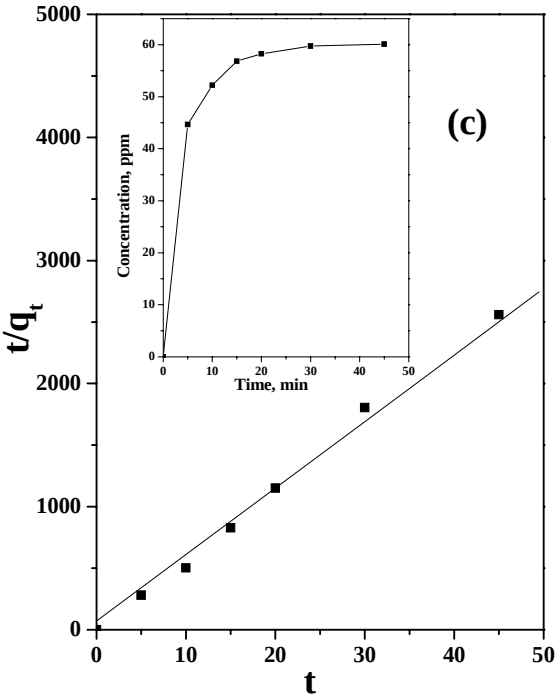

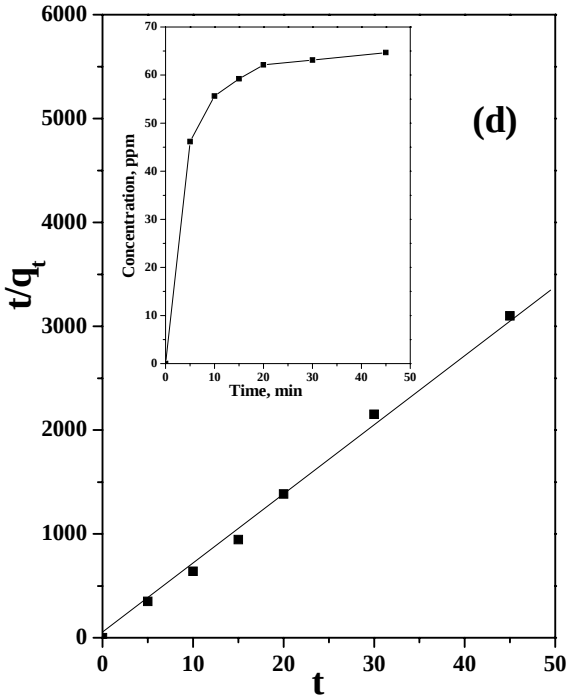

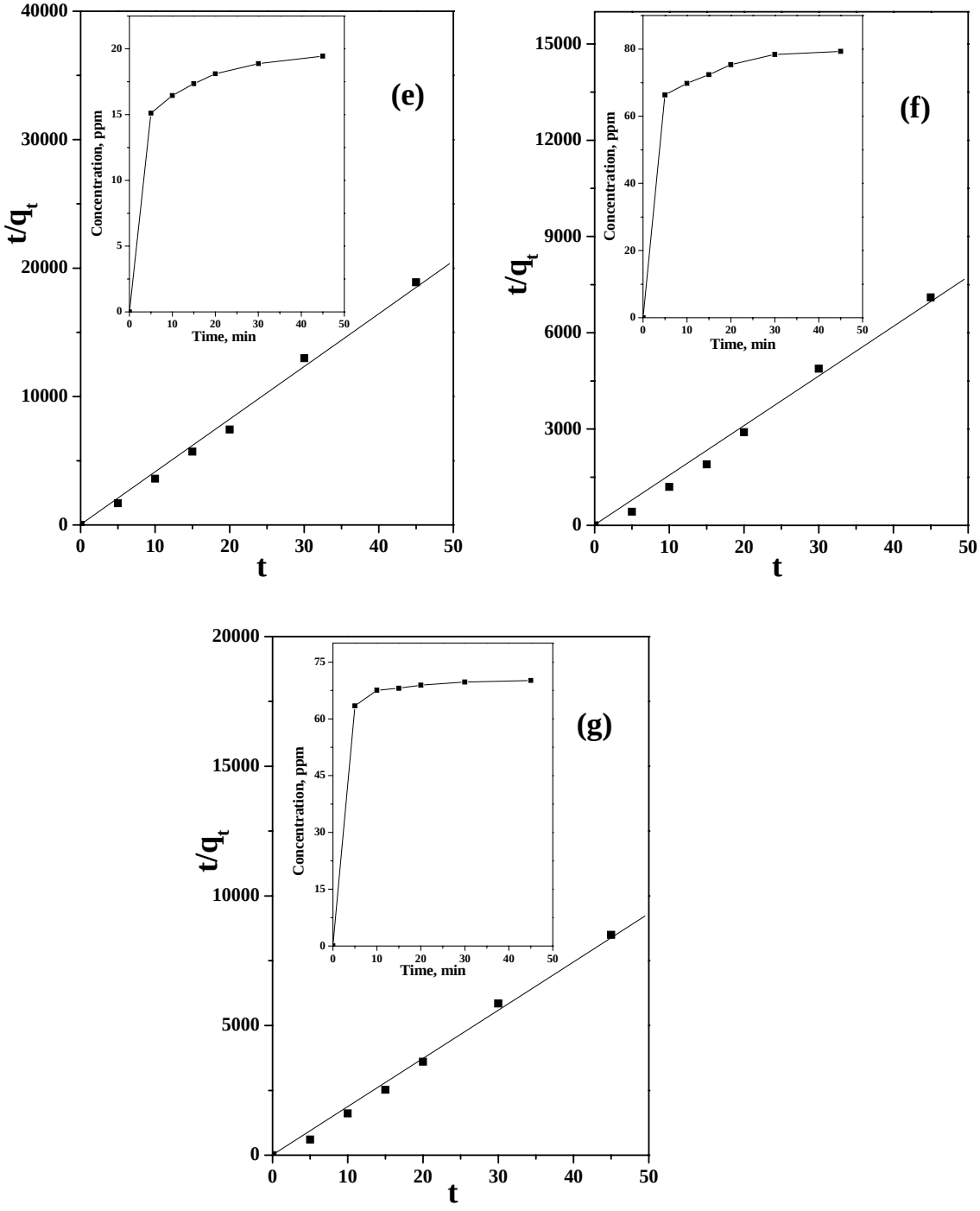

Fig. S12. The linear plot of desorbed dye concentration with the function of time for different sulfonated dyes (a) OG, (b) CR, (c) CB, (d) MO, (e) CRR (f) ARS and (g) CBB for 2 g/l of **II**. Inset shows the increase of concentration of the respective dyes with variation of time.

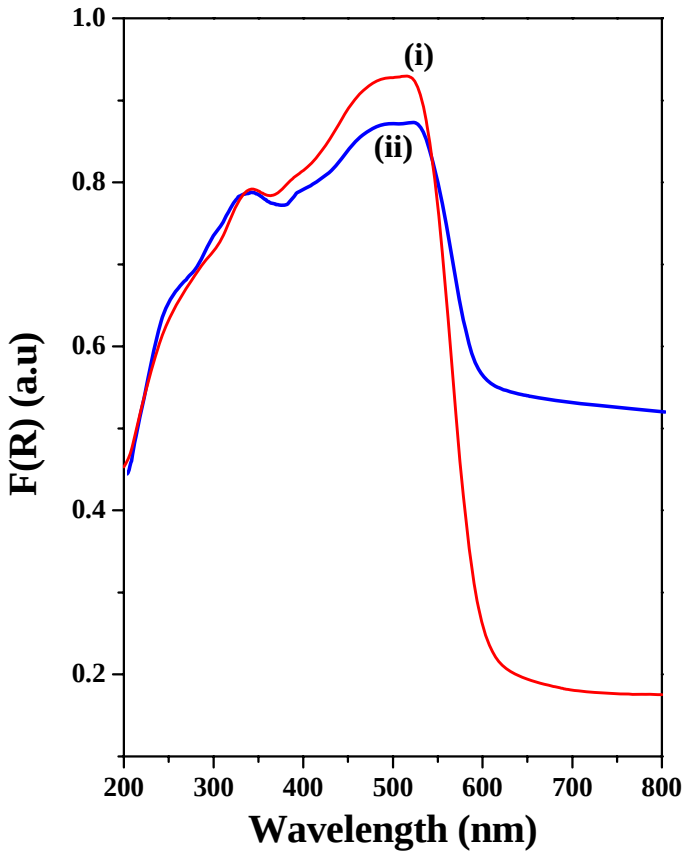

Fig. S13. Solid state UV-vis absorbance like spectra for (i) OG adsorped compound **II** (ii) after desorption of OG adsorped compound **II.**

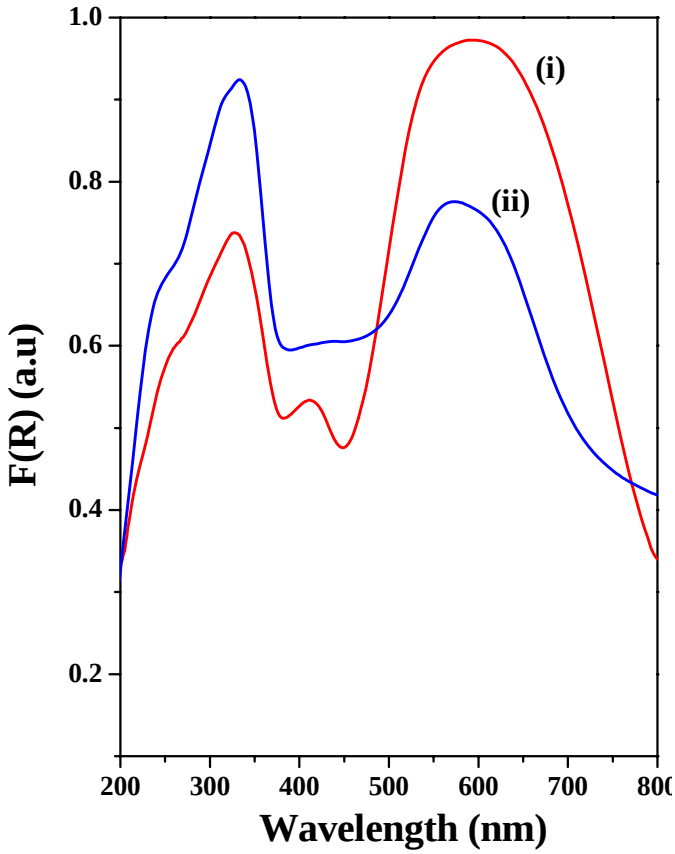

Fig. S14. Solid state UV-vis absorbance like spectra for (i) CBB adsorped compound **II** (ii) after desorption of CBB adsorped compound **II.**

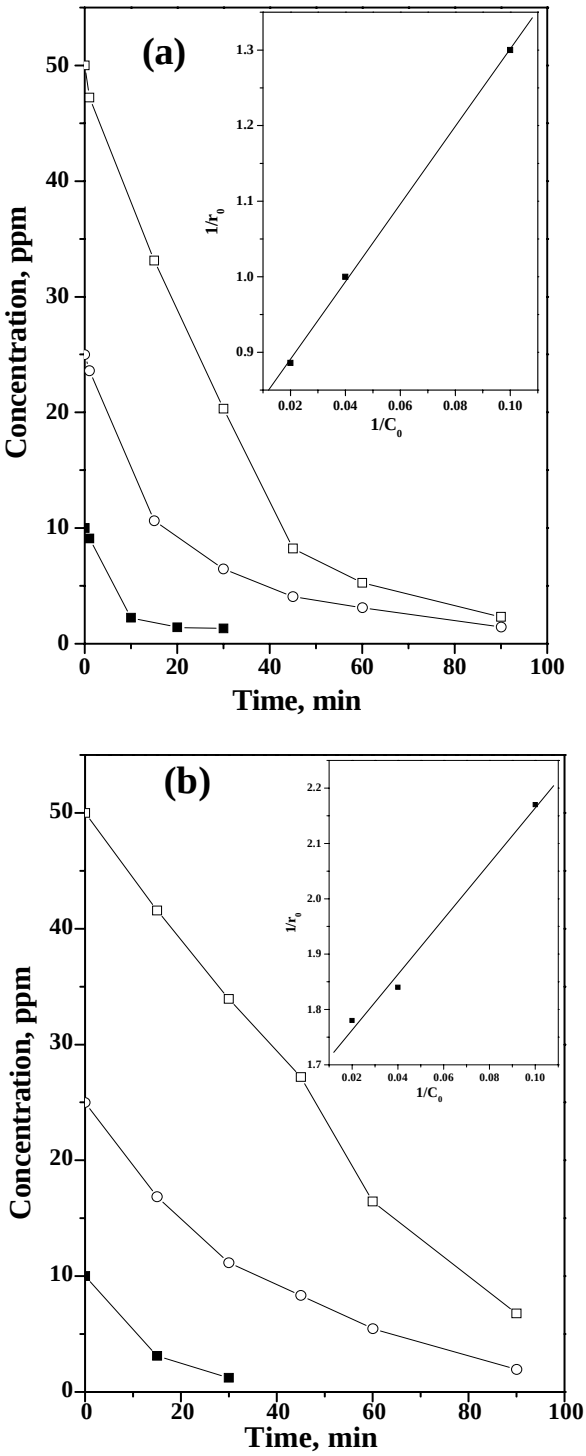

Fig. S15. Degradation profile of different initial concentrations of MB in the presence of (a) **I** and (b) **III** (2 g/l) under UV light (□ = 50 ppm, o = 25 ppm, ■ = 10 ppm). Inset shows the rate of the degradation of MB for corresponding compounds.

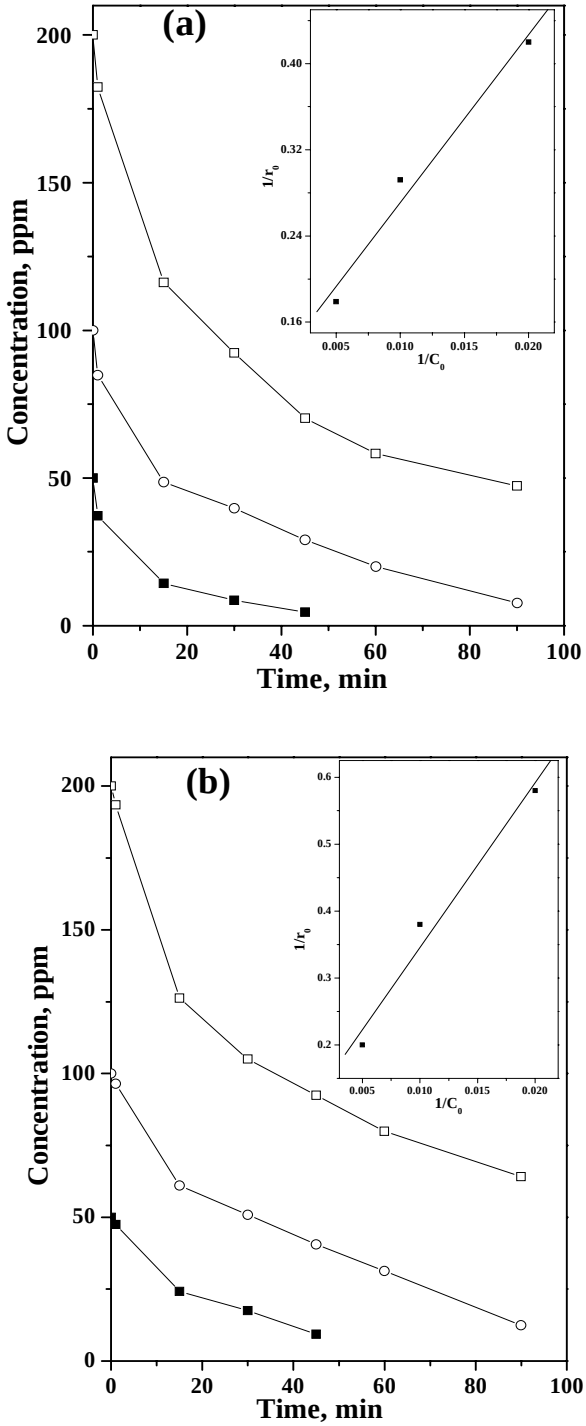

Fig. S16. Degradation profile of different initial concentrations of RBL in the presence of (a) **I** and (b) **III** (2 g/l) under UV light (□ = 200 ppm, o = 100 ppm, ■ = 50 ppm). Inset shows the rate of the degradation of RBL for corresponding compounds.

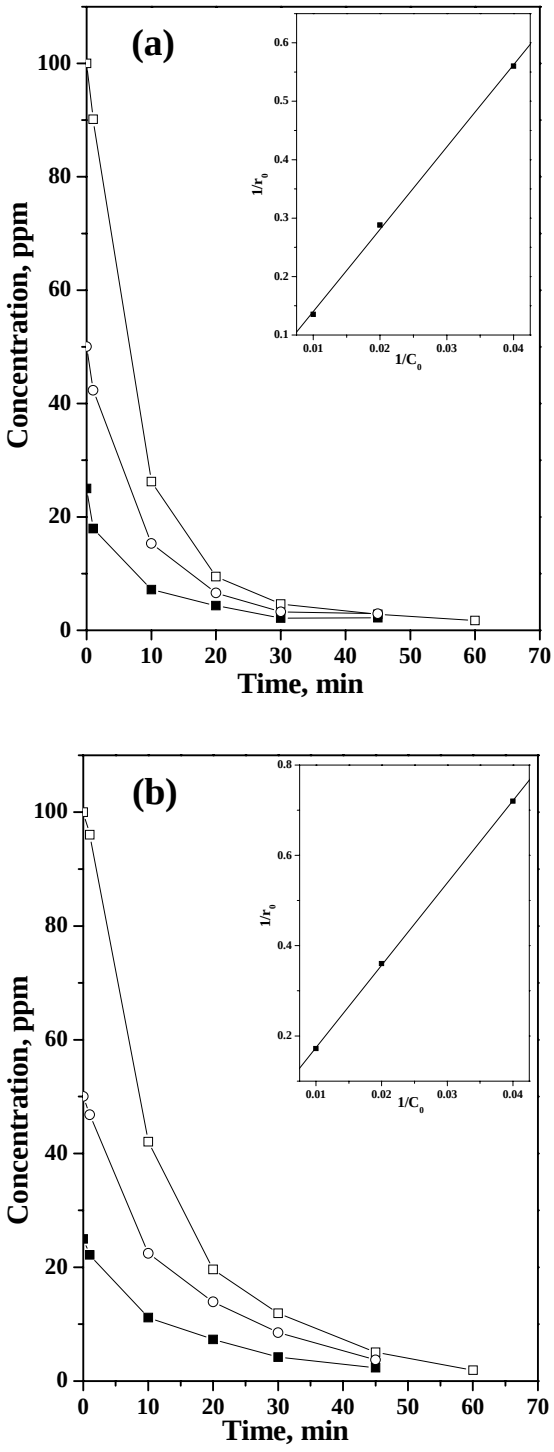

Fig. S17. Degradation profile of different initial concentrations of MV in the presence of (a) **I** and (b) **III** (2 g/l) under UV light (□ = 100 ppm, o = 50 ppm, ■ = 25 ppm). Inset shows the rate of the degradation of MV for corresponding compounds.

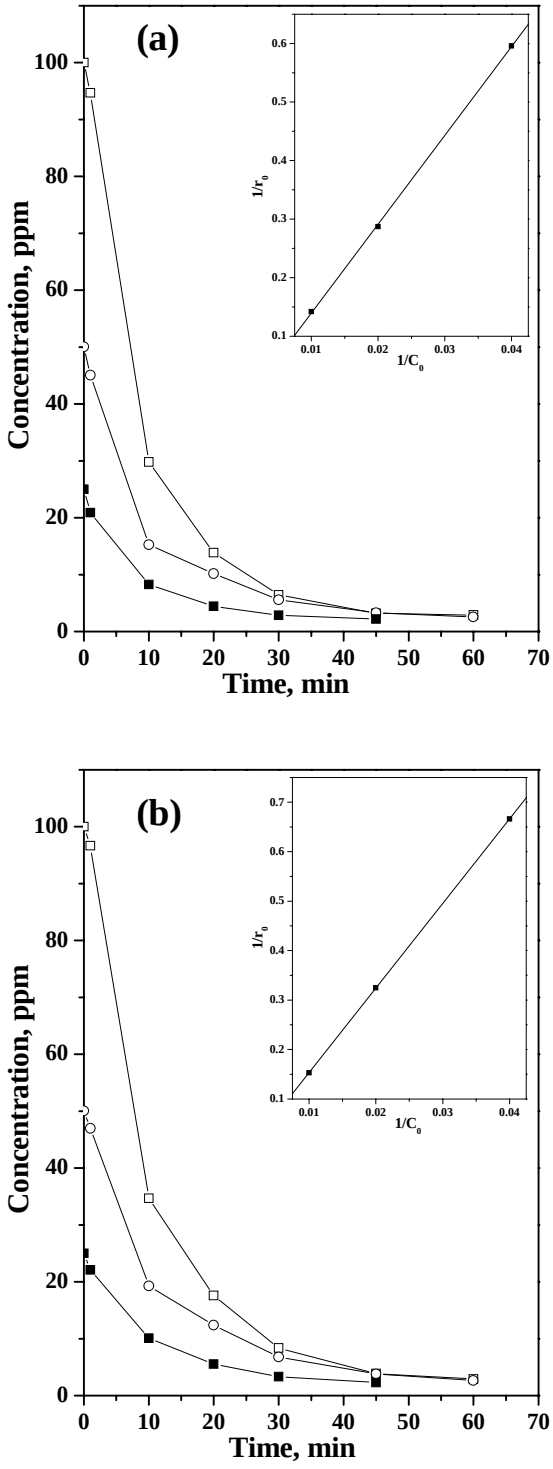

Fig. S18. Degradation profile of different initial concentrations of MR in presence of (a) **I** and (b) **III** (2 g/l) under UV light (□ = 100 ppm, o = 50 ppm, ■ = 25 ppm). Inset shows the rate of the degradation of MR for corresponding compounds.

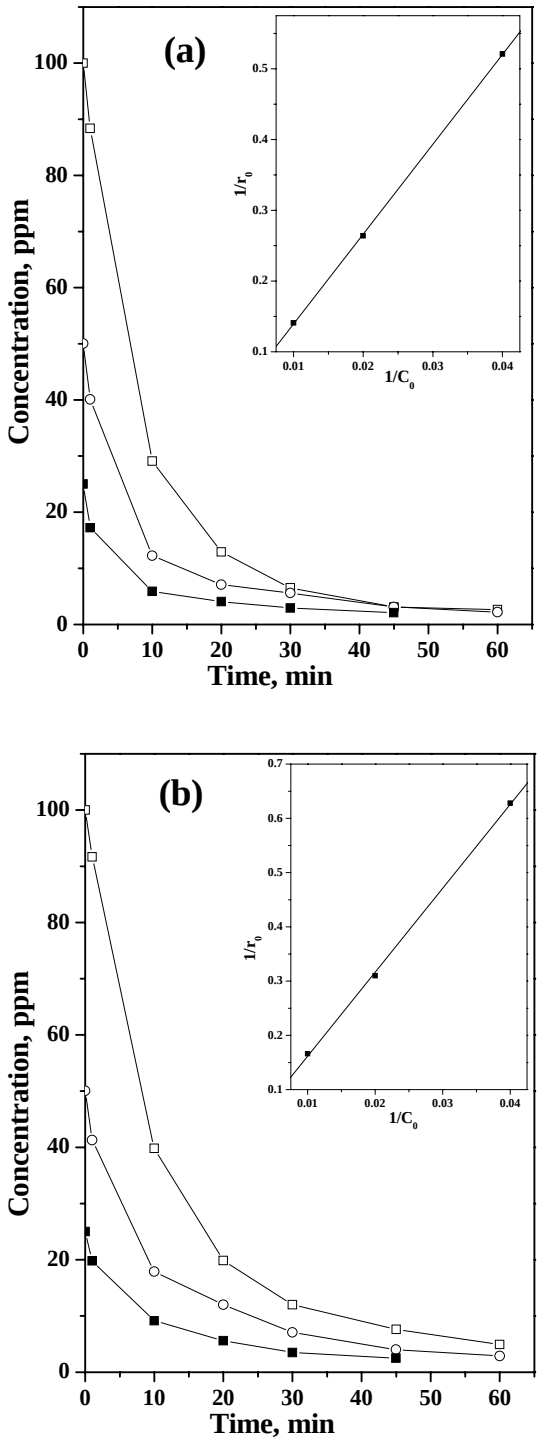

Fig. S19. Degradation profile of different initial concentrations of BBR in the presence of (a) **I** and (b) **III** (2 g/l) under UV light (□ = 100 ppm, o = 50 ppm, ■ = 25 ppm). Inset shows the rate of the degradation of BBR for corresponding compounds.

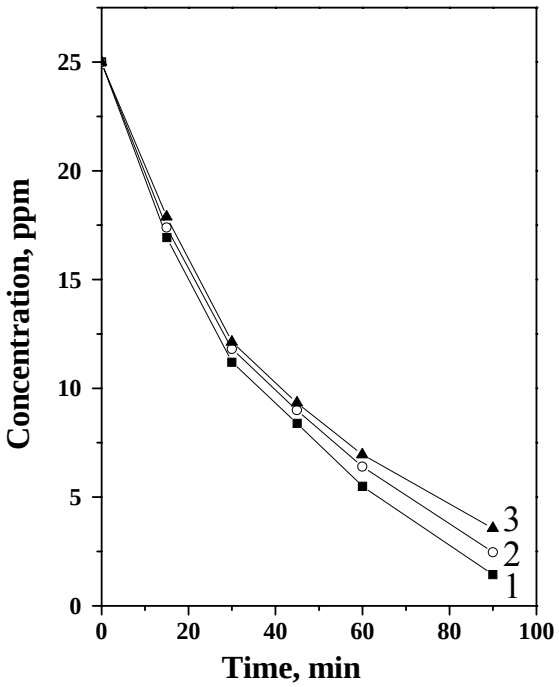

Fig. S20. Degradation profile of MB in the presence of **II** in the repetitive experiment (three times) in the UV-light.

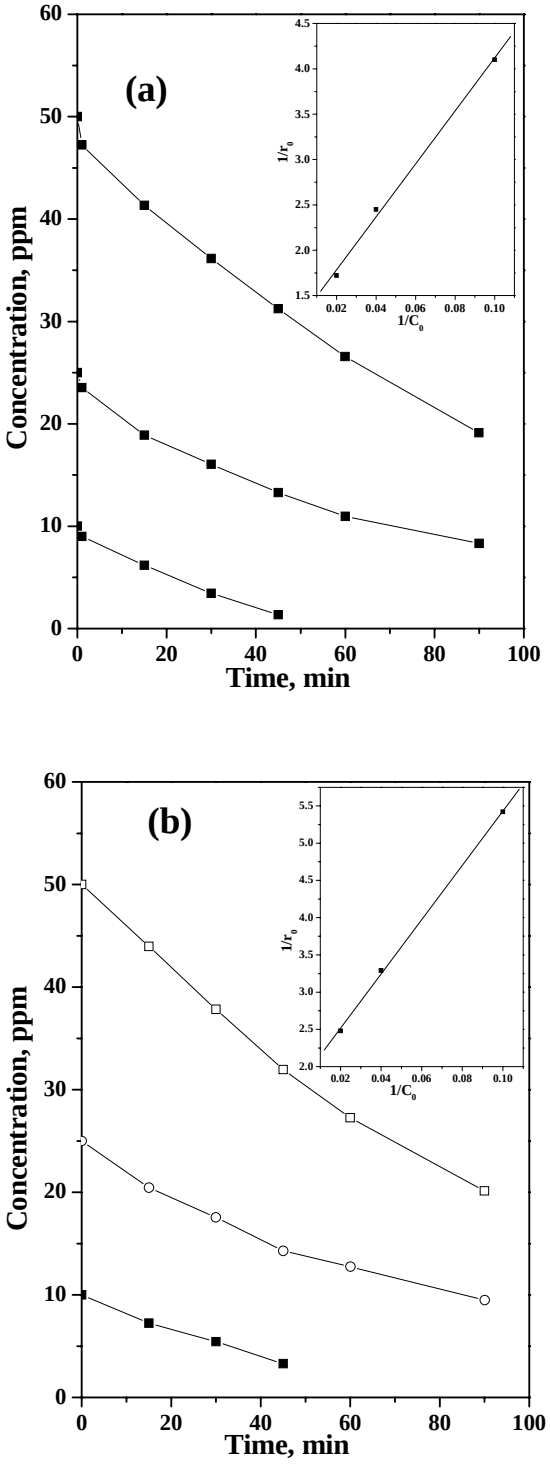

Fig. S21. Sunlight assisted degradation profile of different initial concentrations of MB in the presence of 2 g/l of (a) **I** and (b) **III** (□ = 50 ppm, o = 25 ppm, ■ = 10 ppm). Inset shows the rate of the degradation of MB for corresponding compounds.

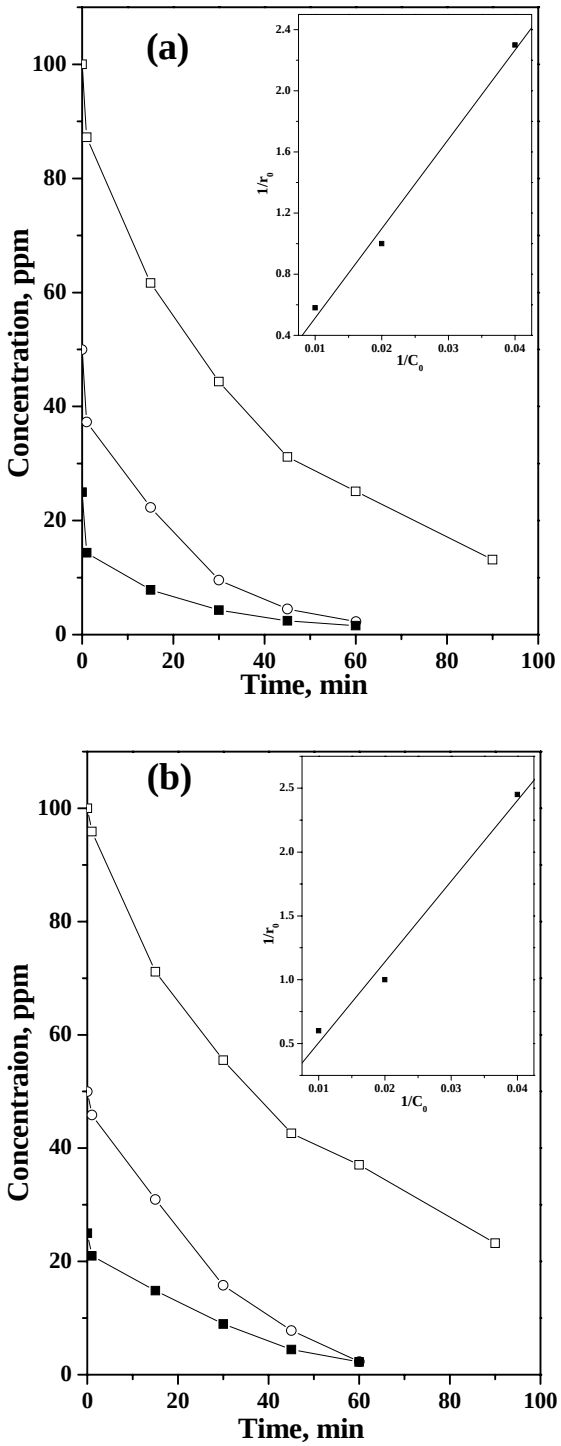

Fig. S22. Sunlight assisted degradation profile of different initial concentrations of RBL in the presence of 2 g/l of (a) **I** and (b) **III** (□ = 50 ppm, o = 25 ppm, ■ = 10 ppm). Inset shows the rate of the degradation of RBL for corresponding compounds.